Characterization of the Lode = -1 Meridian on the Al-2024 Failure Surface for *MAT_224 in LS-DYNA®

Robert L. Lowe, Jeremy D. Seidt, and Amos Gilat

Department of Mechanical & Aerospace Engineering, The Ohio State University, Columbus, OH 43210, USA

Abstract

*A key ingredient in the modeling of ductile fracture using *MAT_224 in LS-DYNA is the failure surface, a 3-D graphical representation of the equivalent plastic strain at failure as a function of stress triaxiality and Lode parameter. Ballistic impact experiments used to validate the existing *MAT_224 plasticity and failure models for 2024 aluminum reveal a strong trend of ductile fractures along the Lode = -1 meridian, a region currently underpopulated with experimental data. Exploiting a novel physical interpretation of the Lode = -1 meridian, several new experiments to populate this critical region are proposed and numerically simulated in LS-DYNA, based on adaptations of the standard ASTM quasi-static hemispherical punch test.*

Introduction

*MAT_224, also known as *MAT_TABULATED_JOHNSON_COOK, is an elastic-viscoplastic material model for ductile metals in LS-DYNA that incorporates stress-state-dependent failure [1,2]. A key ingredient in modeling ductile failure within *MAT_224 is the failure surface, a 3-D graphical representation of the equivalent plastic strain at failure as a function of stress triaxiality and Lode parameter. Recent experimental and theoretical studies confirm the importance of including both triaxiality and Lode parameter dependence in ductile fracture models, particularly when the state of stress is shear-dominated [3-14]. The failure surface in *MAT_224 is calibrated for a particular material using a hybrid numerical-experimental program involving numerous specimen geometries (e.g., plane stress, plane strain, axisymmetric) and loadings (e.g., tension, compression, shear), with each combination characterizing a unique point on the failure surface; see, for instance, Refs. [12,15].

2024 aluminum is a structural metal that is commonly employed in aircraft components. Accurately simulating the failure modes of impacted 2024 aluminum targets in ballistic impact experiments [16] is a necessary first step toward numerically simulating full-scale aircraft engine debris containment events [12]. This, in turn, requires accurate and robust material models for 2024 aluminum. Toward this end, an extensive experimental program was conducted by Seidt and Gilat [12,17] to characterize the elasto-plastic deformation and failure of 2024 aluminum. The resulting experimental data was used by Buyuk [15] to calibrate the *MAT_224 material model (constitutive plus failure) in LS-DYNA for 2024 aluminum.

Ballistic impact experiments [16] used to validate the resulting *MAT_224 plasticity and failure models for 2024 aluminum revealed a strong trend of ductile fractures along the Lode = -1 meridian [11]. Currently, this critical region of the failure surface is underpopulated with experimental data. In this paper, to enable the design of novel experiments to populate this

region of interest, we first demonstrate that states of stress along the Lode = -1 meridian can be physically interpreted as a competition between in-plane equi-biaxial tension and out-of-plane compression. By tuning the ratio of in-plane equi-biaxial tension to out-of-plane compression, we traverse along the Lode = -1 meridian between these two limits, sampling all possible states of stress in between, with triaxialities ranging from -2/3 (pure equi-biaxial tension) to 1/3 (pure uniaxial compression). Exploiting this novel interpretation of the Lode = -1 meridian, several new experiments are proposed and numerically simulated in LS-DYNA, based on adaptations of the standard ASTM quasi-static hemispherical punch test.

Physical Interpretation of the Lode = -1 Meridian on the Failure Surface

We consider a three-dimensional state of stress that consists of in-plane equi-biaxial tension and out-of-plane compression, i.e.,

$$\boldsymbol{\sigma} = \begin{bmatrix} 1 & 0 & 0 \\ 0 & 1 & 0 \\ 0 & 0 & b \end{bmatrix} \sigma_{xx}, \tag{1}$$

with $\sigma_{xx} > 0$. In Eq. (1), the dimensionless parameter

$$b = \frac{\sigma_{zz}}{\sigma_{xx}} \leq 0 \tag{2}$$

quantifies the competition between out-of-plane compression and in-plane equi-biaxial tension. As shown in Table 1, by tuning the parameter *b*, we generate states of stress that traverse the Lode = -1 meridian from pure equi-biaxial tension ($b = 0$) to pure uniaxial compression ($b = -\infty$); see also Ref. [11]. Note that for the triaxiality σ^* and Lode parameter μ we use the definitions

$$\sigma^* = \frac{p}{\sigma_{vm}}, \qquad \mu = \frac{27}{2}\frac{J_3}{\sigma_{vm}^3}, \tag{3}$$

where *p* is the hydrostatic pressure (or mean stress), σ_{vm} is the von Mises equivalent stress, and J_3 is the third invariant of the deviatoric stress tensor.

Stress ratio *b*	Triaxiality	Lode parameter
0	-2/3	-1
-1/2	-1/3	-1
-1	-1/6	-1
-2	0	-1
-5	1/6	-1
-∞	1/3	-1

Table 1: By tuning the stress ratio b, we can adjust the ratio of out-of-plane compression to in-plane equi-biaxial tension and sample a wide range of triaxialities along the Lode = -1 meridian.

Design of Experiments in LS-DYNA to Populate the Lode = -1 Meridian on the Al-2024 Failure Surface in *MAT_224

In this section, we propose two different experiments with different ratios of out-of-plane compression to in-plane equi-biaxial tension at the location of initial failure. As such, they promise to characterize two different points along the Lode = -1 meridian of the Al-2024 failure surface. Both tests are essentially adaptations of the standard ASTM quasi-static hemispherical punch test [18], a classical experiment used to assess the formability of sheet metals in equi-biaxial stress states.

Stress analyses are performed in LS-DYNA. Our metrics for a "successful" design include (a) obtaining targeted values of triaxiality and Lode parameter, (b) maintaining these targeted values over the duration of the simulation, particularly as damage begins to accumulate, and (c) avoiding designs where the boundary conditions strongly influence the deformation physics.

Proposed Test 1: Small-Diameter Quasi-Static Hemispherical Punch Test

A schematic of the setup for a standard ASTM quasi-static hemispherical punch test can be found in [18]. In the adaptation proposed here, we employ (i) a 2.25-mm-diameter hemispherical punch composed of hardened tool steel, (ii) a fixture (clamp + die) composed of Inconel with a 51-mm-diameter circular hole, and (iii) a 1.27-mm-thick disk-shaped specimen composed of 2024 aluminum.

In our modified test, the ratio of the punch diameter to the die diameter is about 1:23, almost 20 times less than the standard ASTM setup of 7:8 [18]. Our rationale for a small punch-to-die ratio is to encourage initial failure near the back center of the aluminum disk, at the point of maximum displacement, where a state of nearly equi-biaxial tension exists throughout the duration of the experiment. Additionally, a small punch-to-die ratio minimizes the influence of the die/clamp boundary conditions on the deformation physics of the aluminum disk, which can be difficult to model and quantify accurately in a numerical simulation.

A 3-D CAD drawing of the proposed experimental design was developed in Autodesk Fusion 360® and meshed in Altair HyperMesh®. To simplify the model, the fixture (clamp + die) is modeled as a concentric ring tied to the outer surface of the aluminum disk, accomplished using the Equivalence Nodes feature in HyperMesh. The specimen and fixture are discretized using 3-D constant-stress 8-node solid hex elements (ELFORM = 1). The punch is discretized using 2-D Belytschko-Tsay 1-point quad shell elements (ELFORM = 2) with three through-thickness integration points (NIP = 3). The *CONTROL_HOURGLASS card (with hourglass formulation IHQ = 6) is included in the LS-DYNA input deck to account for the tendency of under-integrated elements to hourglass. Overall, our model contains over 1.02 million elements, with a characteristic element size of about 100 microns.

In our LS-DYNA finite-element model, the punch material (hardened tool steel) and fixture material (Inconel) are modeled using *MAT_20, a rigid material model. The specimen material (2024 aluminum) is modeled using *MAT_224, a tabulated Johnson-Cook material model, calibrated for Al-2024 by Buyuk [15] using the experimental data of Seidt and Gilat [12,17]. The punch is prescribed a constant speed of 500 mm/s (small enough to avoid introducing inertial

effects, but large enough to ensure a reasonable run time for the simulation) using the *BOUNARY_PRESCRIBED_MOTION_RIGID card. The motion of the fixture is constrained using the CON1 and CON2 constraint parameters in *MAT_20. Automatic surface-to-surface contact is employed at the specimen/punch interface, with SOFT = 2 segment-based contact.

The simulation terminated normally in just over 49 hours using a shared-memory parallel (SMP) version of LS-DYNA running on 8 CPUs. Contour plots reveal a concentrated buildup of damage at the center of the back surface of the specimen (i.e., the location of maximum deflection), driven by large in-plane equi-biaxial tensile stresses arising due to membrane stretching. Accordingly, element erosion (failure) first occurs at this location. Simultaneously, a substantial buildup of shear and compression occurs near the leading edge of the specimen-punch contact zone. After failure on the back surface and subsequent relief of the in-plane equi-biaxial tensile stresses, these regions of large shear and compression quickly accumulate damage, leading to circumferential cracking and the ejection of a plug (see Figs. 1a and 1b).

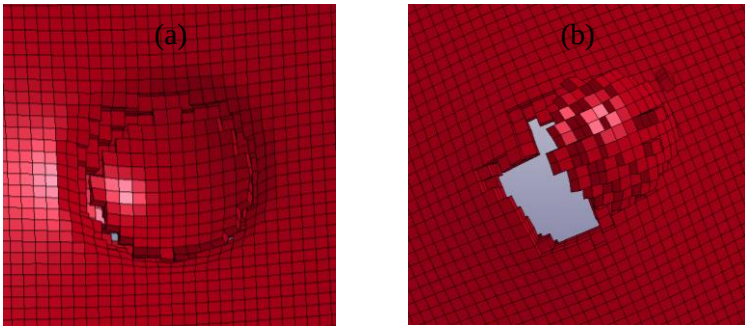

Figure 1: Initial element erosion at the center of the back surface of the specimen gives way to (a) circumferential cracking on the top surface and (b) plug ejection.

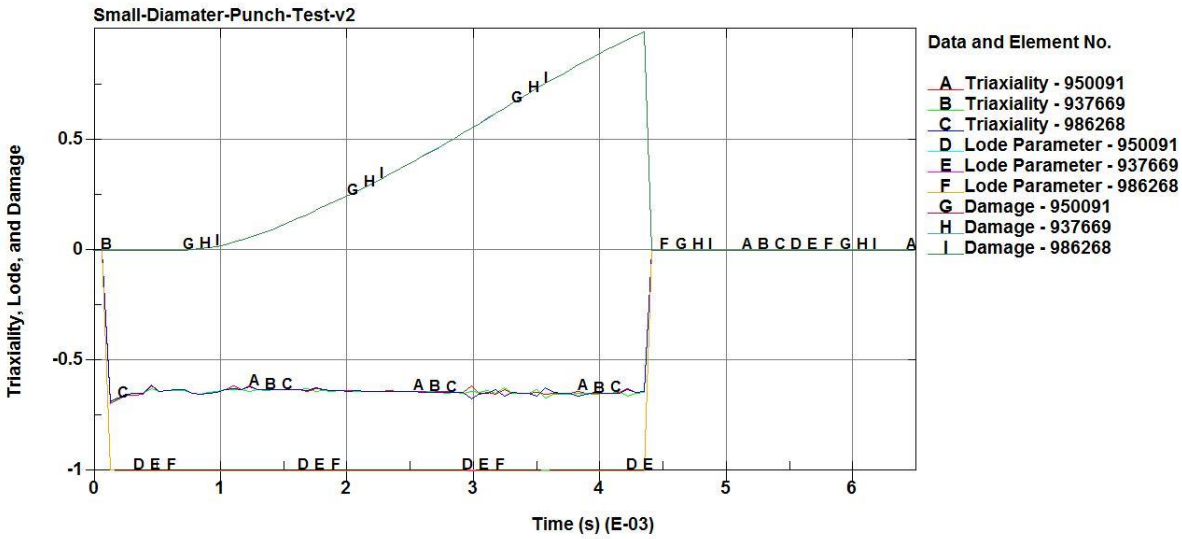

Figure 2: Triaxiality, Lode parameter, and damage histories in the first elements to erode in the specimen. The average triaxiality is about -0.64 during damage accumulation. The Lode parameter remains steady around -1 as damage accumulates, prior to initial failure at t = 4.39 ms.

At the first elements to fail, history plots of the stress components reveal a state of stress that is predominantly in-plane equi-biaxial tension. Contour plots reveal that the triaxiality and Lode parameter are uniform in a roughly 1-2 mm diameter zone at the back center of the specimen. The Lode parameter remains relatively constant at -1 until first failure at 4.39 ms (see Fig. 2). The average triaxiality is around -0.64, i.e., nearly pure equi-biaxial tension (see Fig. 2).

Proposed Test 2: Small-Diameter Quasi-Static Hemispherical Punch Test with Backing Plate

A schematic of the setup for a standard ASTM quasi-static hemispherical punch test can be found in [18]. In the adaptation proposed here, we employ (i) a 2.25-mm-diameter hemispherical punch composed of hardened tool steel, (ii) a fixture (clamp + die) composed of Inconel with a 25.4-mm-diameter circular hole, (iii) a 1.27-mm-thick disk-shaped specimen composed of 2024 aluminum, and (iv) a 1.27 mm-thick disk-shaped backing plate composed of annealed copper. Note that the ratio of the punch diameter to the die diameter is about 1:11, almost 10 times less than the standard ASTM setup of 7:8 [18]. Our rationale for a small punch-to-die ratio is to minimize the influence of the die/clamp boundary conditions on the deformation physics of the aluminum disk, which can be difficult to model and quantify accurately in a numerical simulation. Perhaps more importantly, a small punch-to-die ratio encourages initial failure near the back center of the aluminum disk, at the point of maximum displacement, where the state of stress is a combination of in-plane equi-biaxial tension (due to membrane stretching) and out-of-plane compression (due to the resistance of the backing plate).

Annealed copper is chosen as the backing plate material for two reasons. First, annealed copper is more ductile than 2024 aluminum, which encourages the specimen to fail first, before the backing plate. Second, annealed copper is lower in strength than 2024 aluminum, which encourages initial failure at the bottom center of the specimen rather than the punch contact zone at the top of the specimen. The latter is more likely to occur when the backing plate material is higher in strength than 2024. This is because in the high-strength limit, the backing plate tends toward a rigid surface, leading to a state of pure uniaxial compression at the back center of the specimen, which is unfavorable for damage accumulation and failure. Conversely, in the low-strength limit, the backing plate tends toward a free surface, leading to substantial membrane stretching and a state of equi-biaxial tension at the back center of the specimen, favorable conditions for rapid damage accumulation and failure (refer to Proposed Test 1).

Exploiting the 2-D axisymmetric nature of the problem, a CAD drawing of a 2-D cross section (or "slice") of the proposed 3-D experimental design was developed in Autodesk Fusion 360® and meshed in Altair HyperMesh®. To further simplify the model, the fixture (clamp + die) is modeled as a concentric ring tied to the outer surface of the aluminum and copper disks using the Equivalence Nodes feature in HyperMesh. The specimen, punch, fixture, and backing plate are discretized using axisymmetric solid elements (ELFORM = 15 in *SECTION_SHELL) with three through-thickness integration points (NIP = 3). The *CONTROL_HOURGLASS card (with hourglass formulation IHQ = 6) is included in the LS-DYNA input deck to account for the tendency of under-integrated elements to hourglass. Overall, our model contains over 15,000 elements, with a characteristic element size of about 50 microns.

In our LS-DYNA finite-element model, the punch material (hardened tool steel) and fixture material (Inconel) are modeled using *MAT_20, a rigid material model. The backing plate

material (annealed copper) is modeled using *MAT_24, a piecewise linear plasticity model, calibrated for annealed copper using data from MatWeb (www.matweb.com). The specimen material (2024 aluminum) is modeled using *MAT_224, a tabulated Johnson-Cook material model, calibrated for Al-2024 by Buyuk [15] using the experimental data of Seidt and Gilat [12,17]. The punch is prescribed a constant speed of 500 mm/s (small enough to avoid introducing inertial effects, but large enough to ensure a reasonable run time for the simulation) using the *BOUNARY_PRESCRIBED_MOTION_RIGID card. The motion of the fixture is constrained using the CON1 and CON2 constraint parameters in *MAT_20. 2-D automatic surface-to-surface contact is employed at the punch/specimen and specimen/backing-plate interfaces.

The simulation terminated normally in just under 40 minutes using a shared-memory parallel (SMP) version of LS-DYNA running on 15 CPUs. Contour plots reveal a concentrated buildup of damage at the center of the back surface of the specimen, the location of maximum deflection (see Fig. 3a). This damage accumulation is driven primarily by large in-plane equi-biaxial tensile stresses due to membrane stretching and, to a lesser extent, out-of-plane compressive stresses due to the interaction with the backing plate. Ultimately, element erosion (failure) first occurs at this location (see Fig. 3a). Simultaneously, a substantial buildup of shear and compression occurs at the top of the specimen near the leading edge of the contact zone. After failure on the bottom surface, these regions quickly accumulate damage, leading to circumferential cracking and the ejection of a plug (see Figs. 3b and 3c).

At the first element to fail, history plots of the stress components reveal a competition between in-plane equi-biaxial tension and out-of-plane compression, dominated by the former. This is also reflected in an average triaxiality of about -0.53 (see Fig. 4). Note that the triaxiality evolves only modestly after the damage accumulates beyond 10% (see Fig. 4); only these values of triaxiality are included in the average. The Lode parameter remains relatively constant at -1 until the element erodes at 2.2 ms (see Fig. 4). Contour plots reveal that the triaxiality and Lode parameter are uniform in a roughly 1-2 mm diameter zone at the center of the specimen.

Summary

Several modifications of the standard ASTM quasi-static hemispherical punch test were proposed and numerically simulated in LS-DYNA. Our numerical simulations revealed that the proposed experimental designs are promising candidates for populating the Lode = -1 meridian on the Al-2024 failure surface, a region of high interest in aerospace-related ballistic impact events. The first test uses a small punch-to-die ratio to encourage failure in a state of nearly equi-biaxial tension (average triaxiality of -0.64) at the back center of the specimen. The second test employs a similar setup, with the addition of an annealed copper backing plate. The introduction of out-of-plane compressive stresses (due to the interaction with the backing plate) reduces the average triaxiality to -0.53 in the first element to erode in the specimen.

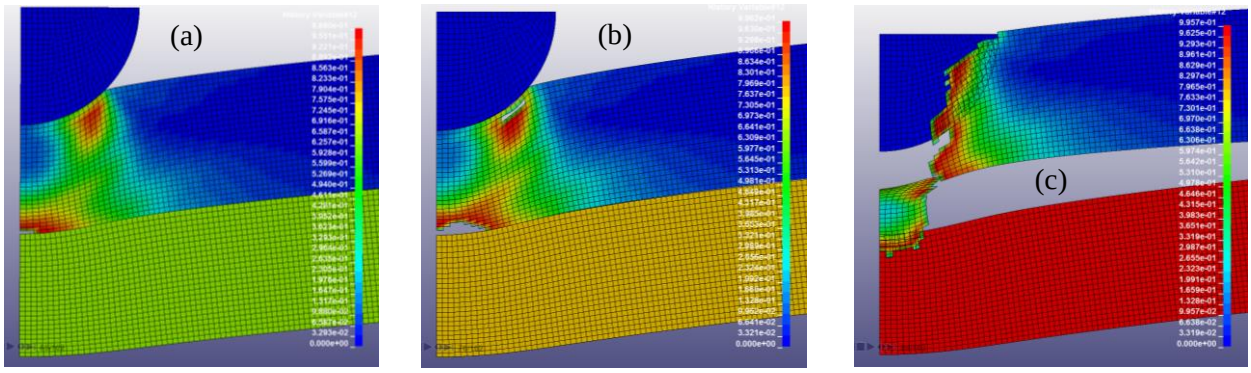

Figure 3: Damage evolution in the 2024 aluminum specimen. (a) Initial failure at the bottom surface at t = 2.2 ms. (b) Secondary crack formation near the contact zone at t = 2.6 ms. (c) The secondary circumferential crack propagates downward and a plug shears off at t = 3.0 ms.

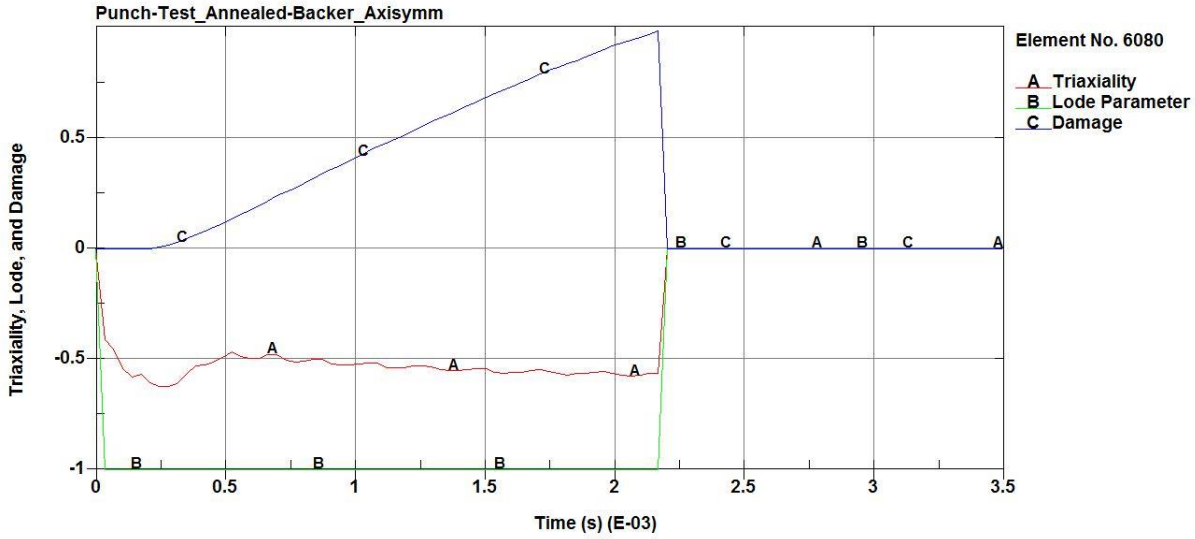

Figure 4: Triaxiality, Lode parameter, and damage histories in the first element to erode in the specimen. The average triaxiality is about -0.53 during damage accumulation. The Lode parameter remains steady around -1 as damage accumulates, prior to initial failure at t = 2.2 ms.

Acknowledgments

This work was funded by Federal Aviation Administration (FAA) grant 11-G-003; thanks to Bill Emmerling and Chip Queitzsch for their support and involvement. We gratefully acknowledge Kelly Carney and Paul DuBois for numerous helpful conversations. We also thank C.K. Park of the Center for Collision Safety and Analysis at George Mason University for supplying the calibrated *MAT_224 constitutive model for Al-2024 used in our LS-DYNA simulations. We gratefully acknowledge the use of high-performance computing resources provided by the Department of Mechanical & Aerospace Engineering at Ohio State.

References

[1] Hallquist, J.O., LS-DYNA Keyword User's Manual, Volume II, 2015.

[2] LS-DYNA Aerospace Working Group, *MAT_224 User Guide, 2015.

[3] Zhang, K.S., Bai, J.B., and Francois, D., Numerical analysis of the influence of the Lode parameter on void growth, *International Journal of Solids and Structures*, 38(32-33), pp. 5847-5856, 2001.

[4] Kim, J., Gao, X., and Srivatsan, T.S., Modeling of void growth in ductile solids: effects of stress triaxiality and initial porosity, *Engineering Fracture Mechanics*, 71(3), pp. 379-400, 2004.

[5] Gao, X. and Kim, J., Modeling of ductile fracture: significance of void coalescence, *International Journal of Solids and Structures*, 43(20), pp. 6277-6293, 2006.

[6] Barsoum, I. and Faleskog, J., Rupture mechanisms in combined tension and shear – experiments, *International Journal of Solids and Structures*, 44(6), pp. 1768-1786, 2007.

[7] Barsoum, I. and Faleskog, J., Rupture mechanisms in combined tension and shear – micromechanics, *International Journal of Solids and Structures*, 44(17), pp. 5481-5498, 2007.

[8] Xue, L., Damage accumulation and fracture initiation in uncracked ductile solids subject to triaxial loading, *International Journal of Solids and Structures*, 44(16), pp. 5163-5181, 2007.

[9] Bai, Y. and Wierzbicki, T., A new model of metal plasticity and fracture with pressure and Lode dependence, *International Journal of Plasticity*, 24(6), pp. 1071-1096, 2008.

[10] Nahshon, K. and Hutchinson, J.W., Modification of the Gurson Model for shear failure, *European Journal of Mechanics A/Solids*, 27(1), pp. 1-17, 2008.

[11] Carney, K.S., DuBois, P.A., Buyuk, M., and Kan, S., Generalized, three-dimensional definition, description, and derived limits of the triaxial failure of metals, *ASCE Journal of Aerospace Engineering*, 22(3), pp. 280-286, 2009.

[12] Seidt, J.D., Plastic Deformation and Ductile Fracture of 2024-T351 Aluminum under Various Loading Conditions, Ph.D. Thesis, The Ohio State University, 2010.

[13] Danas, K. and Ponte Castaneda, P., Influence of the Lode parameter and the stress triaxiality on the failure of elasto-plastic porous materials, *International Journal of Solids and Structures*, 49(11-12), pp. 1325-1342, 2012.

[14] Hutchinson, J.W. and Tvergaard, V., Comment on "Influence of the Lode parameter and the stress triaxiality on the failure of elasto-plastic porous materials" by K. Danas and P. Ponte Castaneda, *International Journal of Solids and Structures*, 49(23-24), pp. 3484-3485, 2012.

[15] Buyuk, M., Development of a Tabulated Thermo-Viscoplastic Material Model with Regularized Failure for Dynamic Ductile Failure Prediction of Structures under Impact Loading, Ph.D. Thesis, The George Washington University, 2013.

[16] Pereira, J.M., Revilock, D.M., Ruggeri, C.R., Emmerling, W.C., and Altobelli, D.J., Ballistic impact testing of aluminum 2024 and titanium 6Al-4V for material model development, *ASCE Journal of Aerospace Engineering*, 27(3), pp. 456-465, 2014.

[17] Seidt, J.D. and Gilat, A., Plastic deformation of 2024-T351 aluminum plate over a wide range of loading conditions, *International Journal of Solids and Structures*, 50(10), pp. 1781-1790, 2013.

[18] ASTM E643-15 Standard Test Method for Ball Punch Deformation of Metallic Sheet Material, ASTM International, West Conshohocken, PA, 2015.